Numerical modeling of solid phase microextraction: binding matrix effect on equilibrium time

Md. Nazmul Alam[1], Luis Ricardez-Sandoval[2], Janusz Pawliszyn[1]*,

[1*]Department of Chemistry, University of Waterloo, Waterloo, Ontario, N2L 3G1, Canada

[2]Department of Chemical Engineering, University of Waterloo, Waterloo, N2L 3G1, Canada

Phone: 1-519-888-4567 ext. 84641. Fax: 1-519-746-0435. E-mail: janusz@sciborg.uwaterloo.ca.

Abstract

Solid phase microextraction (SPME) is a well-known sampling and sample preparation technique used for a wide variety of analytical applications. As there are various complex processes taking place at the time of extraction that influence the parameters of optimum extraction, a mathematical model and computational simulation describing the SPME process is required for experimentalists to understand and implement the technique without performing multiple costly and time-consuming experiments in the laboratory. In this study, a mechanistic mathematical model for the processes occurring in SPME extraction of analyte(s) from an aqueous sample medium is presented. The proposed mechanistic model was validated with previously reported experimental data from three different sources. Several key factors that affect the extraction kinetics, such as sample agitation, fiber coating thickness, and the presence a binding matrix component, are discussed. More interestingly, for the first time, shorter or longer equilibrium times in the presence of the binding matrix component were explained with the help of an asymptotic analysis. The parameters that contribute to the variation of the equilibrium times are discussed assuming one binding matrix component present in a static sample. Numerical simulation results show that the proposed model captures the phenomena occurring in SPME, leading to a clearer understanding of this process. Therefore, the currently presented model can be used to identify optimum experimental parameters without the need to perform a large number of experiments in the laboratory.

……

Key words: solid phase microextraction, mathematical model, numerical simulation, binding matrix effects

Introduction

Solid phase microextraction (SPME) has already been recognized by the scientific and industrial community as a powerful alternative sampling and sample preparation technique to technologies such as liquid-liquid or solid phase extraction, as is evidenced by its rapid growth over the past decades.[1] The theory and practice of SPME have been examined in considerable detail in recent years in order to facilitate the processes of learning and application of this relatively new technique.[2] In SPME, a small amount of extracting material (usually polymeric) is dispersed onto a solid support to create an open-bed extraction phase. When the solid-supported extraction media is exposed to an analytical sample for a period of time, the extraction yield is primarily dependent on the partitioning of analyte(s) between the sample bulk phase and the supported extraction phase. The partitioning is in turn dominated by the physicochemical factors related to the analyte, the sample matrix (i.e., the part of sample other than the analyte), and the extraction phase. Based on the total residence time of the extraction phase in the sample solution, two extraction methods are used: (i) equilibrium extraction, which refers to extractions that take place when the extraction amount does not change significantly, or when partition equilibrium is reached and, (ii) non-equilibrium extraction, which is the extracted amount at any given time before a state of equilibrium is reached. The extraction processes in SPME consist of several physical domains with several processes occurring simultaneously, i.e., diffusion, convection, matrix binding, and adsorption or absorption.[3] Different research groups have proposed slightly different approaches to model the kinetics of the absorption process for SPME. For example, some groups[4,5] considered the SPME fiber as a one-compartment, first-order kinetic model, whereas our group[2] divided the uptake process into two parts: intra-fiber molecular diffusion in the coating domain, and mass

transfer around the fiber, which is governed by intra-layer molecular diffusion over a stagnant layer with a finite thickness. Hermens' group modified the later approach by introducing the mass transfer coefficient as a leading force due to the concentration gradient between the bulk medium and the fiber surface.[6] Nevertheless, all these models have been simplified such that an analytical solution for the proposed model can be obtained; this can cause difficulties for experimentalists seeking to implement them in developing practical SPME methods that can be realistically applied to actual systems. Moreover, quantification of freely dissolved analytes with SPME under non-equilibrium conditions can be erroneous due to the influence of matrix components in the kinetic regime of extraction.[7] Some studies reported an increased analyte uptake rate in the presence of matrix during the kinetic phase of extraction.[8] The plausible explanation for this enhanced kinetics is known as the "diffusion layer effect".[7] Conversely, other studies reported unaltered uptake kinetics in the presence of matrix.[9] Although the majority of the reports agree with the fact that the matrix can affect the uptake kinetics only if the extraction is limited by the diffusion in the boundary layer, a lack of understanding remains regarding the effect of the physical parameters on the transport kinetics in a complex matrix.

In spite of all the developments achieved in different aspects of SPME, from the creation of different formats to its expansion of applications, it still remains a challenge for experimentalists to readily determine suitable experimental conditions that can provide acceptable (optimal) extraction amounts at low analyte concentrations. As such, the development of a computational model will help increase our current knowledge of SPME methods by providing insight into the nature and dynamic characteristics of the extraction process [10] In addition, the utilization of a computational model would significantly decrease the time and labor needed to develop and test

several SPME designs as compared to the current practice of performing multiple (expensive) experiments.

In this work, a computational-based mechanistic model for the absorption processes occurring in SPME has been developed using the finite element analysis software, COMSOL MULTIPHYSICS™. Several common SPME experimental parameters, such as effect of agitation, fiber coating thickness and the presence of a binding matrix component were considered and tested with the proposed model. The mechanistic model presented in this study is able to provide insight into how physical parameters affect the extraction kinetics of an analyte from a binding matrix component-containing sample. A set of general guiding principles that were adapted from an asymptotic analysis[11] were used as a predictive tool to achieve desired uptake kinetics or to explain the experimental extraction time profile for a complex matrix. The mechanistic model was validated with previously published experimental data obtained from different sources.

Experimental Section

Mathematical model

The present model involves three simultaneous and coupled processes: fluid flow past the SPME fiber dipped in the sample to be analyzed, mass transport to and from the fiber coating, and absorption of analyte by the fiber coating. Each of the domains considered in the present model is described next.

In the present mechanistic model, a typical geometry of SPME sampling was set up based on the experimental configurations reported by Louch *et al.*,[12] where the sample was placed in a vial stirred with a magnetic stirrer, which provided convective flow, and the SPME fiber was

inserted through the vial cap. A schematic representation of the sample vial and SPME fiber, along with the corresponding modeling domain, is depicted in Figure 1a. The fiber was located away from the center of the vial in order to avoid the central vortex region and to satisfy the assumption that the fluid flows past the fiber with a velocity normal to the fiber axis.[13] The present analysis assumes a simple 2D geometry (Figure 1b) for simplicity of modeling and in order to reduce the amount of necessary calculations. The xy plane is set to be the cross-section of the sample container, whereas the x-axis is set to be along the direction of flow. The governing equations for the fluid flow, the mass transport, and the matrix effect are described next.

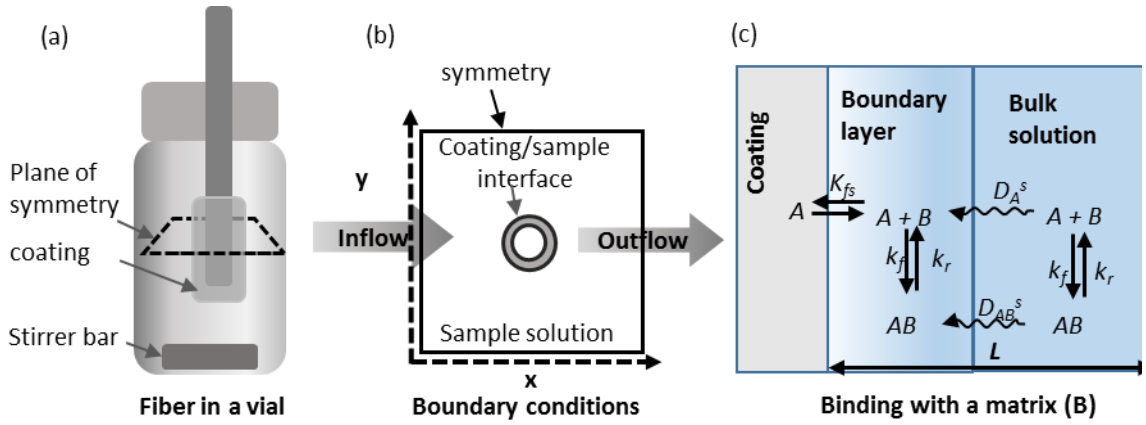

Figure 1. Schematic representation of the SPME/sample configuration. Experimental geometry based on Louch *et al.* containing a magnetic stirrer mediated convection, (a).[12] Here, a silica rod is used as a support for the coating, which is immersed in a sample solution for direct extraction. The 2D geometry with the boundary conditions used in the model, (b). A schematic diagram of the transport processes occurring in each region in the presence of a binding matrix component (*B*), (c). An analyte (*A*) binds with *B* with forward and reverse rate constants (k_f) and (k_r), respectively. Both the free or bound analytes can diffuse to the boundary layer with diffusivities D_A^s and D_{AB}^s, respectively. It is assumed that only the analyte can be absorbed into the coating with a distribution constant of K_{fs}.

Fluid flow equations

Since the flow in the sampling container of SPME is in a low Reynolds number condition, it is assumed to be a laminar flow. The Navier-Stokes equation was employed to model the fluid

flow in the sampling container. The conservation of momentum for incompressible fluid flow in a 2D geometry can be formulated as follows:

$$\rho\frac{\partial u}{\partial t}+\rho\left(u\frac{\partial u}{\partial x}+v\frac{\partial u}{\partial y}\right)-\mu\nabla^2 u+\frac{\partial p}{\partial x}=0 \quad (1)$$

$$\rho\frac{\partial v}{\partial t}+\rho\left(u\frac{\partial v}{\partial x}+v\frac{\partial v}{\partial y}\right)-\mu\nabla^2 v+\frac{\partial p}{\partial y}=0 \quad (2)$$

Where u and v are the velocity components in the x and y directions, respectively; ρ is the fluid density, p is pressure and μ is the fluid viscosity. For incompressible fluid flows, the following continuity equation is also considered:

$$\frac{\partial u}{\partial x}+\frac{\partial v}{\partial y}=0 \quad (3)$$

The boundary conditions for the fluid flow model are shown in Figure 1(b). Symmetry conditions $\left(\frac{\partial u}{\partial x}=\frac{\partial v}{\partial y}=0\right)$ were set at the two edges (Figure 1b). The boundary condition at the outlet was set to $p = 0$. A linear velocity was set at the inlet of the geometry. In order to obtain the linear velocity from stirring the solution with a magnetic stir bar, the following equation was employed: [2]

$$u(x)=0.575\,\pi NR^2\frac{1}{x} \quad (4)$$

Where R is the radius of the stir bar and N represents the revolutions per second.

Mass transport equations

The analyte is transported by diffusion and convection in the bulk solution, whereas diffusion is the only transport mechanism occurring in the fiber coating. According to Fick's law,

the following mass balances can be formulated to describe the time-dependent mass transport model for the present system[14]:

$$\frac{\partial C_A^s}{\partial t} + \nabla.(-D_A^s \nabla C_A^s + C_A^s \boldsymbol{U}) = 0 \quad (5)$$

$$\frac{\partial C_A^f}{\partial t} + \nabla.\left(-D_A^f \nabla C_A^f\right) = 0 \quad (6)$$

Where $C_A{}^s$ and $C_A{}^f$ denote the concentrations (mol m^{-3}) of the analyte *A* in the solution phase and fiber coating, respectively. $D_A{}^s$ is the diffusivity coefficient (m^2s^{-1}) in the solution phase, and $D_A{}^f$ is the diffusivity coefficient (m^2s^{-1}) in the fiber coating, while $\boldsymbol{U}$ denotes the velocity field, which can be obtained from the Navier-Stokes model described in the previous section. Equation (5) is valid for the solution side where convection is applied, whereas equation (6) is for the fiber's domain, where only diffusion is assumed to occur. At the coating/solution boundary, the conditions that ensure continuity of the dependent variables in the two regions, i.e., fiber coating and aqueous solution, need to be specified.[15] As schematically shown in the supplementary information in Figure S1 the fluxes at the boundary are coupled using Newton's law type expressions:

$$-D_A^f \frac{\partial C_A^f}{\partial x} = M(C_A^s - K_{fs} C_A^f) \quad (7)$$

$$-D_A^s \frac{\partial C_A^s}{\partial x} = M(K_{fs} C_A^f - C_A^s) \quad (8)$$

Where *M* is an arbitrary parameter called the stiff-spring velocity term, which should be of a large enough value so that a considerable mass exchange between the two regions can be established. This technique has been used in previous studies that consider mass transfer between two different media.[16,17] K_{fs} is called partition coefficient. When a liquid phase is in contact with a

solid phase, the K_{fs} can be defined as the ratio of the concentration of a species in the solid phase to that in the liquid phase where they come in contact ($K_{fs} = C_A^f/C_A^s$).[2]

A specified inlet concentration equal to the initial concentration was set at the inlet boundary ($C_A^s = C_A^{s,0}$) and vanishing of $\partial C_A^s/\partial x^2$ at the outlet. The following equality of the mass flux of the analyte was considered at the sample vessel wall:

$$(C_A^s \boldsymbol{U} - D_A^s \nabla C_A^s) = 0 \quad (9)$$

Equations for a binding matrix component

When a binding matrix component is present, (e.g., humic organic matter in a water sample), the association and dissociation between the freely dissolved analytes and the binding matrix in the sample domain can be expressed as follows:

$$A + B \rightleftarrows AB \quad (10)$$

Where *A* is the freely dissolved analyte, *B* represents the binding matrix component, and *AB* is the bound species. The present study assumes that the fiber coating absorbs only analytes in a matrix-containing sample and follows the same physics as described in the previous section "mass transport equations". In the solution domain, simple binding kinetics between analyte and matrix were used to model the influence of the matrix on the extraction of analyte (i.e. second-order forward and first-order backward).[18] The modeled experimental systems involved addition of bovine serum albumin or humic acids to water samples, as previously reported in the literature.[19,20] The model parameters used in this study are shown in Table S1, found in the

supplementary information. The transport of the species in the sample is schematically shown in Figure 1c.

The rates of association (k_f) and dissociation (k_r), commonly expressed as the dissociation constant (K_D), determine the strength of the affinity interaction (Equation (11)), which regulates analyte release from the bound matrix into the sample media.

$$K_D = \frac{k_r}{k_f} = \frac{C_A . C_B}{C_{AB}} \tag{11}$$

Here, C_A, C_B, and C_{AB} are the molar concentrations of the free analyte in the sample, the free matrix component (e.g., humic acid), and the bound matrix component, respectively.

The mass transport within the sample can be described using mass balances for the free analyte and the analyte-bound matrix component. The concentration of free analyte (C_A) at the diffusion boundary layer changes with respect to the diffusion from the sample, as well as association or dissociation with the bound matrix, i.e.,

$$\frac{\partial C_A}{\partial t} = \nabla . (D_A \nabla C_A) - k_f C_A \left(C_{B,T} - C_{AB}\right) + k_r C_{AB} \tag{12}$$

where $C_{B,T}$ is the concentration of total matrix added.

The concentration of complex (C_{AB}) relies only on the equilibrium binding,

$$\frac{\partial C_{AB}}{\partial t} = k_f C_A \left(C_{B,T} - C_{AB}\right) + k_r C_{AB} \tag{13}$$

where the concentration of free binding matrix (C_B) is described as the difference between the concentration of total matrix added ($C_{B,T}$) and the concentration of complex (C_{AB}), i.e.,

$$C_B = C_{B,T} - C_{AB} \quad (14)$$

Computational model

COMSOL Multiphysics 4.4, a finite element method (FEM) based software package, was used in this study to analyze the mass transfer processes in SPME. In order to obtain an accurate representation of the SPME system, the time-dependent partial differential equations for each of these physical processes must be solved simultaneously. The procedure used to solve this problem is divided into two steps: (1) determination of the fluid velocity profile at steady-state assuming incompressible flow and (2) use of this steady-state velocity profile as the initial condition to solve for the coupled transient mass transport and absorption equations. The extracted amount at each time point was calculated by multiplying the average concentration in the fiber with its volume. The normalization of extracted amount was carried out by dividing the extracted amount at each time point by the equilibrium quantity.

Results and Discussions

Model validation

Effect of convection on equilibrium time

The mechanistic model developed in this study has been validated with previous experimental work performed by our group for the extraction of benzene from an aqueous solution by a polydimethylsiloxane (PDMS) coating.[12] The model developed in this study can predict the equilibration time with the absence or presence of stirring in the sample solution (shown in Figure

2).The model slightly under estimates the extracted amount for the static condition. Unavoidable convection due to the fiber or solution movement might contribute to the higher extracted amount at each time point. To further validate the model for static condition, a full equilibration time profile for static condition was shown to be well fitted as presented in Figure S2. The equilibration time, 100 seconds, predicted by the present model is in agreement with the experimental data presented in a previous study[12] with stirring speeds as high as 2,500 rpm. Moreover, the simulated results for varying coating thicknesses provided very good fitting with the experimental data, as shown in the supplementary information (Figure S3). The good fitting of the experimental data indicates the coupling between solution and coating phases in the mathematical model both for agitated and non-agitated sample systems.

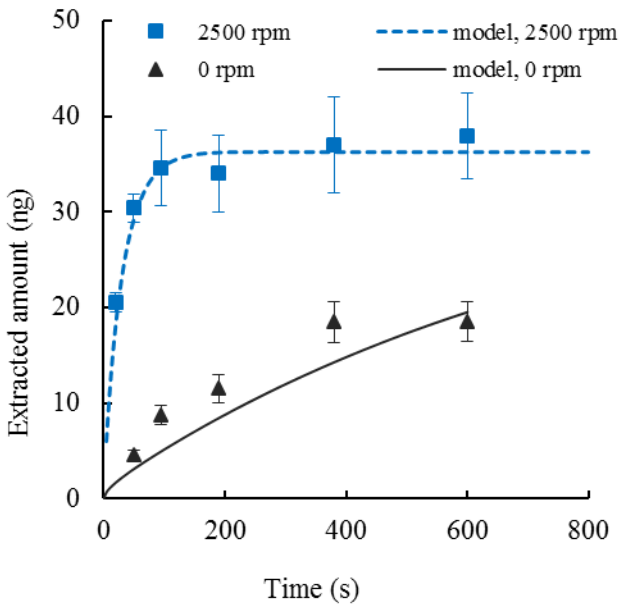

Figure 2. Effect of stirring on the extraction profile of 1 ppm benzene in water extracted with a 56 µm thick PDMS coating. Here, D_A^s: 1.08×10^{-9} m^2/s, D_A^f: 2.8×10^{-10} m^2/s, C_A^s:1 ppm, K_{fs}: 125. The error bars represent standard deviations (n = 3).

Matrix effect on equilibrium time

The matrix effect on the SPME equilibrium time is still not well understood. Here, the proposed mathematical model is employed to explain the mechanism of the kinetics of extraction in presence of matrix in sample. Assumption was made that no significant physical adsorption or partition of matrix components occurs on the surface of the coating. In order to test whether the model can reproduce experimental data for shorter or unaltered equilibrium time, two different experimental set-ups were considered. First, the model was validated with experimental data reported by Hermens *et al.* on the effect of bovine serum albumin (BSA) on uptake kinetics of pyrene from an aqueous sample using a PDMS fiber coating.[19] The experimental and simulated data are shown in Figure 3a. The model predicted the experimental data very well, even at different concentration levels of albumin. In this experimental set-up, the equilibrium time was shorter by the increased concentration of albumin. Another validation of the model is shown in Figure 3b, with the experimental data obtained from Broeders *et al.*[20] The proposed model has been shown to predict experimental data when the time to reach equilibrium was not perturbed while the extracted amount at equilibrium was less in the presence of matrix (albumin) than that of the standard chlorpromazine (analyte) sample. The details on the rate of extraction influenced by the presence of a binding matrix component is discussed in detail in the following sections.

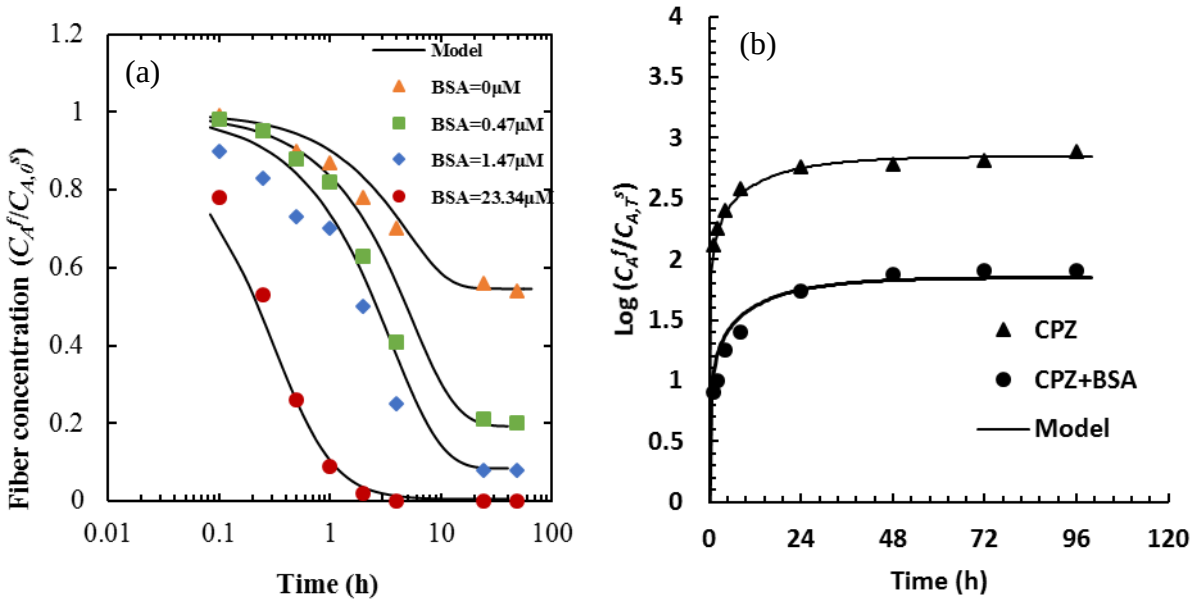

Figure 3. Influence of a binding matrix component (albumin) on the equilibration time. Experimental data from Hermens *et.al.*[19] were fitted with the developed model (a). Here, both the equilibration time and extracted amount were influenced by the presence of albumin in pyrene extraction by PDMS coated fiber. The model simulation fitted with the data from Broeders *et al.*[20] (b). Here, only the extraction amount was influenced by the presence of albumin during the extraction of chlorpromazine by polyacrylate coating (b). The model parameters are presented in supplementary information (Table S1).

Mechanisms of the matrix effects on equilibrium time

The literature review indicates that possible matrix effects on SPME kinetics fall into three different categories. The most common is the reduced equilibrium time that is particularly problematic when the goal is to measure the freely dissolved concentration under non-equilibrium conditions. In other words, calibration of SPME under non-equilibrium conditions would be possible only if the binding matrix containing the sample to be analyzed and the calibration sample (without binding matrix) had identical uptake dynamics. The reduction of equilibration time was typically observed where the amount of extracted analyte by the coating was negligible (usually

less than 5%) compared to the initial amount present in the sample, i.e., the depletion was negligible.[7] The second class of binding matrix effect observed was with sampling systems where a significant quantity of analyte was depleted from the sample solution. While the rate of extraction becomes slower in the binding matrix-containing sample, the extracted amount is almost the same compared to the standard sample.[21] The third class of binding matrix effect pertains to an initial fast extraction followed by a slower rate, which increases the equilibration time with significantly lower extracted amount at equilibrium.[22] With the help of an asymptotic analysis,[11] these three possible scenarios can be described by the present model, and are explained next.

To explanation of the effects of a binding matrix component on uptake kinetics, the physical process of transport under the condition of diffusion-limited extraction is described considering the following three dimensionless parameters:

$$\alpha = \frac{C_A}{C_{B,T}}$$

$$\beta = \frac{L^2 k_r}{D_A^s}$$

$$\gamma = \frac{k_f C_A}{k_r} = \frac{C_A}{K_D}$$

Where α represents the amount of freely dissolved analyte (C_A) at the beginning of the experiment relative to the total amount of binding matrix ($C_{B,T}$). This term is influenced by the K_D of the analyte-matrix pair, since the system is assumed to be initially at equilibrium; therefore, α represents a measure of the free analyte in the sample matrix. The second parameter, β, relates the timescale of analyte diffusion to the timescale of unbinding of the analyte-matrix complex. This term is dependent on the size of the sample container (L), the dissociation rate of the complex (k_r),

and the diffusivity of the analyte through the sample (D_A^s). The third parameter, γ, is the concentration of bound matrix component in the sample relative to the unbound portion at the beginning of the experiment. For $\gamma \gg 1$, most of the binding matrix component are in the bound state initially. Conversely, if $\gamma \ll 1$, only a small fraction of the binding matrix component have bound analytes. This term is governed by K_D and the amount of free analyte at the beginning of an experiment.

Scenario one: shorter equilibrium time; diffusion controlled kinetics

At first, the diffusion-controlled kinetics of SPME was established by increasing the diffusivity of the analyte in the solution and observing the concomitant changes in the extraction time profiles (Figure S4, found in supplementary information). An increase in analyte diffusivity in the solution, from 1×10^{-9} to 5×10^{-6} m^2/s, yielded a substantially faster uptake rate, which supports the diffusion-controlled kinetics hypothesis. All the kinetic studies presented in the following sections were carried out under the condition of diffusion controlled kinetics.

Effect of K_D on uptake kinetics

In order to study the effect of different parameters of extraction, an experimental system using chlorpromazine binding to BSA was considered,[20] where the equilibrium dissociation constant (K_D) was calculated as 5.4×10^{-4} M. The K_D is a measure of binding strength between the analyte and the binding matrix; generally, the higher the hydrophobicity (higher log P), the lower the K_D value for the analyte-binding matrix complex. Please note that a PDMS coating was assumed instead of using a polyacrylamide coating, as the present scenario aims to study extraction under the diffusion-controlled regime. The mathematical model was used to investigate the effect

of K_D on the extraction kinetics, since the kinetics are not sensitive to changes in individual values of k_f and k_r (Figure S5, found in supplementary information). The effect of K_D was studied by varying k_r while keeping k_f constant, since the rate of association tends to be more consistent between binding pairs than the rate of dissociation. Figure 4a shows that the kinetic of extraction is influenced by the strength of the analyte-matrix pair (K_D). Interestingly, K_D values of 10^{-5} and 10^{-6} provided the most significant enhancement in this study. The asymptotic analysis provided that under the condition of diffusion-controlled kinetics, i.e., fast decomplexation ($\beta \gg 1$), and with a small proportion of bound matrix component ($\gamma << 1$), extraction occurs over a single time scale (t_s), according to:

$$t_s = \frac{L^2(\,1 + C_{B,T}/K_D)}{D_A^s} \tag{15}$$

This term demonstrates that the equilibrium time is dependent on the hydrophobicity of the analyte at constant values of $C_{B,T}$, L and $D_A{}^s$. Increasing hydrophobicity under these conditions will lead to a decrease in equilibration time. The model predicts that a weak interaction (10^{-3} M) does not appreciably affect the equilibration time (equilibrium reached at 20 minutes), whereas a strong interaction (10^{-6} M) significantly reduced the time to reach equilibrium, with only 5 minutes needed to reach equilibrium. A weak binding matrix component does not appreciably perturb the kinetics under this condition, although the conditions $\beta >> 1$ and $\gamma << 1$ were pertained in all the cases. It is worthwhile to mention that with the increase of K_D, increasing amount of analyte remains bound to the matrix and therefore the quantity of free analyte becomes less.

In contrast to the above findings, the extraction time profiles at the early stages of extraction show that the uptake rate for the analyte solution without the binding matrix component is the

highest (Figure 5b). The rate also decreases as the binding strength between the analyte and matrix increases. Although the initial uptake rate for the sample solution without matrix is the highest, it takes longest time to reach equilibrium (shown in Figure 5a). We assume that with the decease of free analyte concentration in solution due to progressively stronger binding affinity towards the binding matrix the fiber coating requires lesser amount of analyte to reach equilibrium. For instance, when K_D is equal to 10^{-5} or 10^{-6} the binding matrix buffers the system leading to very low free analyte concentration and consequently reducing the equilibration time. Moreover, the concentration gradient in solution domain extends shorter distance for the high K_D values whereas thicker gradient is obvious for binding matrix free solution as the complex located close to the coating provides required amount of the analyte to reach condition close to equilibrium value (Figure S6). Therefore, equilibration time becomes shorter for binding matrix containing samples compared to the extraction from matrix-free solution, when the concentration is equal to the free concentration in solution containing the binding matrix component.

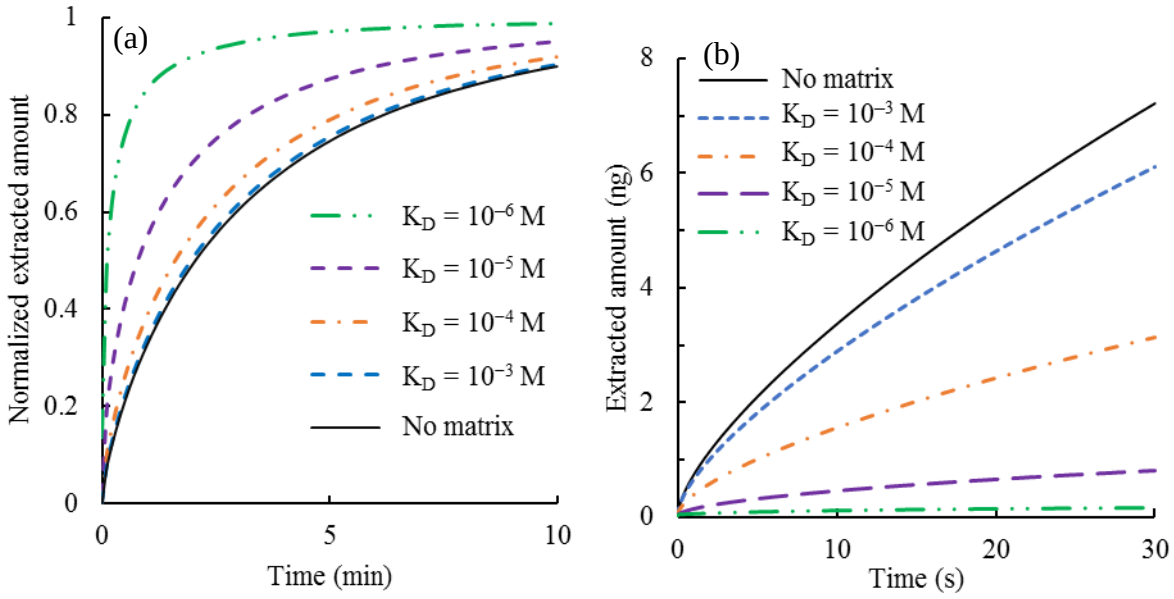

Figure 4. Model simulation of equilibrium time profiles influenced by varying the strength of the binding matrix from weak (K_D = 10^{-3} M) to strong (K_D = 10^{-6} M), for a chlorpromazine to BSA ratio of 1: 2.5, (a). Extracted amount at the initial stage of extraction time profiles, (b). For this study, k_f was kept constant at 1×10^6 M^{-1} s^{-1} and k_r varied to obtain different K_D values. For all values of k_f and k_r, $\beta >> 1$ and $\gamma << 1$. Analyte depletion was assumed negligible (less than 5%) by setting radius of the sampling container (L) at 10 mm which is equivalent to 15 mL of the sample. Moreover, the convection was set zero (static conditions) to assume only diffusion controlled transport of analyte. All other model parameters are presented in Table S1.

Effect of analyte to binding matrix component ratio on equilibrium time

The mathematical model was used to examine the effect of the initial analyte-to-binding matrix component (for example, BSA) ratio, containing both weak and strong bindings, on the reduction or enhancement of the equilibration time. In this case, the analyte concentration was held constant while the BSA concentration was varied. As shown in Figure 5a, for the weak binding complex system (K_D of 5.4 $\times10^{-4}$ M), the simulation results show that an increase in analyte-to-BSA ratio of 1:25 to 1:1000 provides a 25 percent reduction of equilibration time. For the strong

binding complex system (K_D = 5.4 ×10^{-5} M), shown in Figure 5b, a similar range of reduction is achieved using an increase in ratio from only 1: 2.5 to 1:100. This phenomenon can be analyzed using the timescale according to equation (15). If $C_{B,T}/K_D \ll 1$, then the equilibration time is independent of both the matrix concentration and K_D. Therefore, the binding matrix component concentration must be greater than K_D for shorter equilibrium time to obtain. In other words, at a lower ratio of analyte to the binding matrix component, the equilibrium time is barely affected by the matrix, but the effect becomes pronounced as the ratio increases. This also supports the findings from the study of different K_D values presented in previous section that the shorter equilibration time is due to the extraction of less free analytes to attain equilibrium. Ramos *et al.*[23] reported that the binding matrix (humic acids) did not interfere with the determination of the freely dissolved concentration of hydrophobic organics under non-equilibrium SPME with a PDMS coating. Oomen *et al.*[24] indicated that this observed result might be due to the use of a very low concentration of the matrix in the experiment, which produced a lower concentration of bound matrix than that of free analytes. The present mechanistic model with the asymptotic analysis quantitatively explained the required conditions for influencing the equilibrium time.

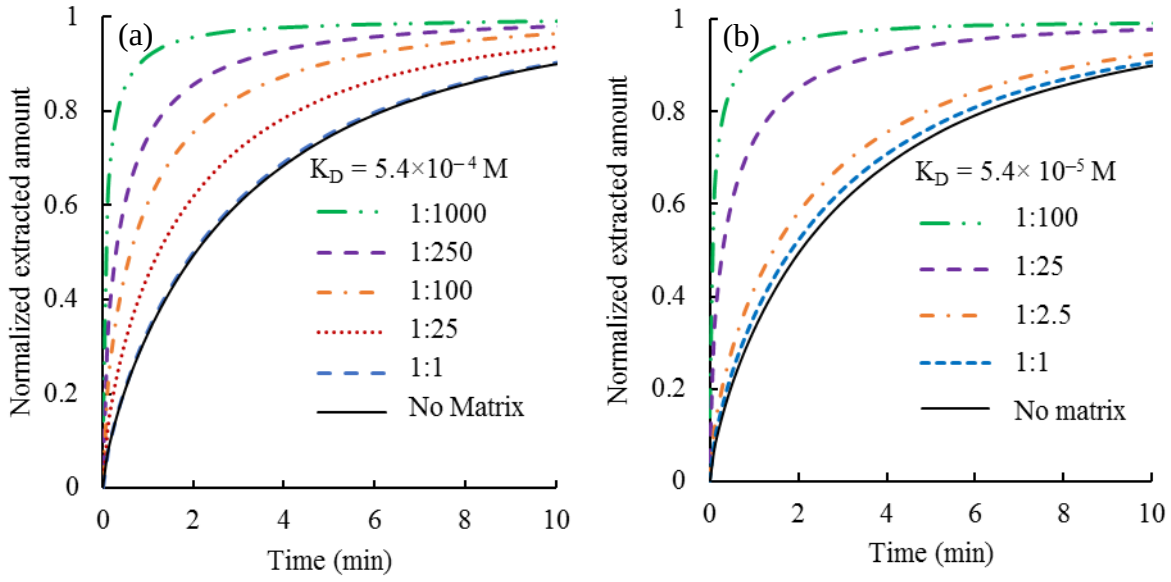

Figure 5. Effect of the ratio of analyte (chlorpromazine) to binding matrix component (BSA) on the extraction kinetics. For weak binding complex, the ration was varied from 1:1000 to 1:1(a) and for strong binding complex the ratio was varied from 1:100 to 1:1 (b). Here, the extent of kinetic enhancement is positively influenced by the strength of the binding partners. The model parameters are presented in Table S1. The convection was set zero (static conditions).

Scenario two: retarded uptake rate; diffusion controlled kinetics

A decrease in uptake rate or longer equilibrium time has been observed in cases where the uptake is still controlled by the diffusion of analyte in solution; however, in such cases, the freely dissolved analyte is locally depleted in the diffusion boundary layer due to the higher amount of extraction by the fiber, i.e., local depletion is significant. In that case analytes need to diffuse from longer distances for the system to reach equilibrium. Porschmann *et al.* reported a retardation in the uptake rate after addition of humic or fulvic acid to a water sample with organotin compounds, i.e. the time to reach equilibrium was increased.[21] Similarly, a retardation of uptake kinetics is observed when smaller sample volumes and lower concentrations of analyte are used compared to the capacity of the SPME coating. For instance, Reyes-Garces *et al.* reported slow uptake rates

for some moderate hydrophobic compounds (for example, metoprolol) in blood plasma samples.[22] This category of binding matrix effect can be explained by the asymptotic analysis and the proposed mathematical model. This type of longer equilibrium is observed when the kinetics are controlled by diffusion ($\beta >> 1$) and when a large proportion of the binding matrix component is bound ($\gamma >> 1$). A two-stage extraction time profile is obtained with the initial timescale of $\frac{L^2}{D_A^s}(1 + \frac{C_{B,T}}{C_A})$. At this stage, the extraction kinetics depends on the total binding matrix concentration ($C_{B,T}$) and the initial free analyte concentration (C_A). The dependency of the initial uptake kinetics with the concentration of free analyte is shown in Figure S7 in the supplementary information. Here the initial uptake rate increases with the decrease of the binding matrix component to analyte ratio whereas the equilibration times remain the same. As the free analyte concentration is depleted until its concentration is equal to K_D, the second stage of extraction starts with a timescale of $\frac{L^2}{D_A^s}(1 + \frac{C_{B,T}}{K_D})$ for the remaining analyte molecules present in the sample. The later timescale is identical to the shorter equilibration time with the binding matrix discussed above in scenario one. For the extraction time profile of binding matrix containing sample, an initial fast extraction is followed by slow diffusion-controlled conditions compared to the one stage and faster equilibration for the binding matrix free solution (Figure 6). The equilibration time is governed by the second timescale which depends on the binding strength (K_D values) between the analyte and binding matrix component. With the increase of binding strength the uptake kinetics are clearly shown to be decreased. Furthermore, the mathematical model was employed to study the concentration profiles in solution domain at different times of extraction under static condition (Figure S8). It is seen that the gradients are stepper for matrix-free standard analyte solution compared to the binding matrix

containing sample. The concentration gradients extend throughout the vial both for binding matrix containing sample and the matrix free solution, unlike to the scenario one where the gradients are thinner for binding matrix containing sample compared to the matrix-free case (Figure S6). Therefore, the mathematical model presented here can be used to predict uptake profiles in cases where the rate is retarded by the local depletion of analyte, but where the kinetics are still diffusion-controlled.

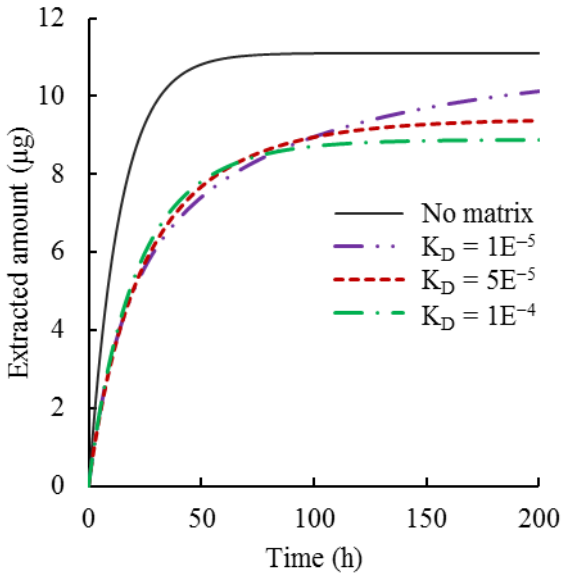

Figure 6. Two stage extraction time profiles with an initial fast uptake kinetics followed by the slow kinetics in the presence of a binding matrix component compared to the single step and faster uptake kinetics for the binding matrix free solution. Here, C_A = 110 µM, $C_{B,T}$ = 100 µM. All other parameters are shown in Table S2. The convection was set zero (static conditions).

Scenario three: retarded uptake rate; analyte dissociation-controlled kinetics

In the third case, the matrix substantially reduces both the uptake rate and the extraction amount at equilibrium. This type of profile was recently reported by Reyes-Garces *et al.* for the extraction of a very hydrophobic analyte, stanozolol (K_D with HSA = 5 E^{-9}M) from a blood plasma sample.[22] From the mathematical analysis and computational simulation, the condition for this

scenario is that the dissociation of bound analyte from the binding matrix is slow compared to the diffusion in solution, i.e., $\beta << 1$ or $\left(\frac{1}{k_r} \gg \frac{L^2}{D_A^s}\right)$. Any free analyte produced by dissociation of the analyte-matrix pair is negligible compared to the existing freely dissolved analytes in the sample solution. As shown in Figure 7, nearly all the freely dissolved analyte is extracted by the coating over the diffusion timescale, L^2/D_A^s. The initial fast diffusive uptake is followed by the slow dissociation of bound analytes over the timescale of $1/k_r$. The uptake rate in the later stage increases with the faster dissociation of analyte from the binding matrix (see Figure S9a). Since analyte diffusivity through environmental or biological samples does not change significantly, either k_r or L needs to be modified for our computational sample system to observe this type of slow kinetics. It is more feasible to modify the diameter of the sample container than the binding kinetics. If the diameter is kept constant at 10 mm, as in the previous simulation experiments, a k_r of $< 10^{-4}\ s^{-1}$ is required for $\beta \approx 1$. This translates to a bound matrix with a half-life of ~3 hours. However, if the vial diameter is sufficiently decreased, it is possible to achieve $\beta \ll 1$ for physically relevant k_r values. More precisely, in order to observe the unbinding-controlled dynamics, the diameter L would need to be below the order of $\sqrt{\frac{D_A^s}{k_r}}$. It was also found that the slower uptake rate is dependent on the extraction capacity of the coating (K_{fs}) when the value of k_r is kept constant (Figure S9b, found in the supplementary information).

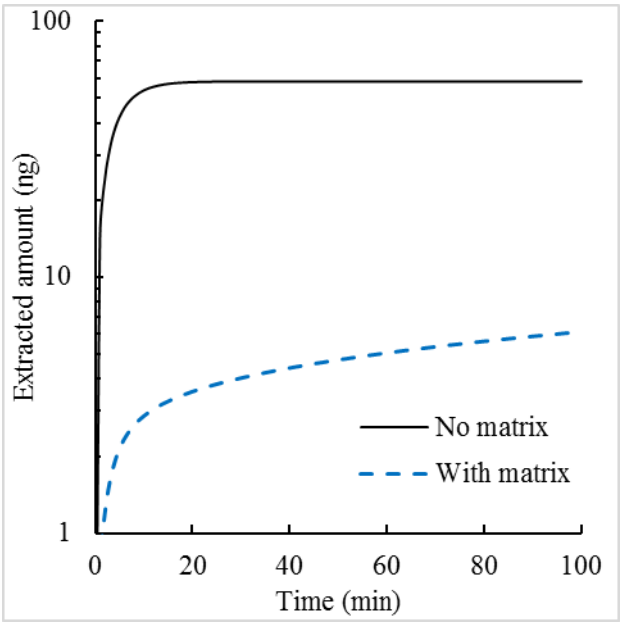

Figure 7. Retardation of uptake kinetics controlled by the L^2/D_A^s in the initial stage followed by the slower stage governed by the dissociation of analyte from the bound matrix component (k_r) compared to the single stage and faster kinetics in the absence of the binding matrix. Here, K_D = 5E^{-9} M and C_A = 5.1 µM, $C_{B,T}$ = 100 µM and L = 1 mm. All other parameters are presented in Table S3. The convection was set zero (static conditions).

The information provided by the above analysis can be used to design an experimental set-up with desired extraction time profiles. In the first scenario, the rate of analyte extraction decreases smoothly over a single timescale. In the other two cases, there are two distinct timescales: an initially fast uptake rate, followed by a more gradual uptake rate. The two timescales in the second case are related, as they are both proportional to L^2/D_A^s, whereas the two timescales in the third case are independently controlled by L^2/D_A^s and k_r, as long as $\alpha \gg \beta\gamma/(\gamma+1)$ and $L \ll \sqrt{\frac{D_A^s}{k_r}}$. Another key difference between the last two cases is that all of the bound analyte molecules remain in the bound state throughout the fast mode for the third case, while approximately half of the bound analyte molecules undergo unbinding in the initial fast stage for the second case. Thus,

the complex sample system can influence not only the timescales of extraction, but also by the amounts of analyte extracted in each stage.

Conclusions

The current work presented a mechanistic-based mathematical model that describes the uptake kinetics in SPME for analytes either from a matrix-free standard solution or a matrix-containing solution. The proposed mathematical model provided excellent prediction of the experimental data available in the literature. The majority of discussion was limited to static conditions, but the conclusions are analogous to cases involving convection. In the case when the convection (e.g. stirring) is present the mass transfer is controlled by diffusion in the boundary layer formed close to the coating surface, not in the whole vial as it is demonstrated in the static case where the boundary layer is equivalent to the size of the vial. It should be emphasized that agitation level will determine the mass transfer rates and the equilibrium value, but in this contribution we focused on binding matrix effects exclusively as they are poorly understood. It was not clear under what experimental conditions the uptake rate is altered with the presence of a binding matrix in sample solution. Now, with the help of this mathematical model and computational simulation, one can easily determine whether the matrix will enhance or retard the uptake kinetics based on the physicochemical properties of the analyte, the matrix, as well as the choice of SPME coating. The modeling has demonstrated that the decrease in equilibration time is not due to increased rate of extraction but due to the requirement of less extracted amount to reach equilibrium, when binding matrix is present. Overall, the simulation results obtained for the present analysis have shown that the present model is a reliable and relatively inexpensive practical method of characterizing the performance of SPME. This model can be used for sample matrices

containing one type of analyte binding components. However, for biomedical application such as human blood or tissue sampling with SPME, further improvement of the model describing the multicomponent phenomena is needed. We are currently extending this study to the application of SPME extraction in tissue or blood sampling. In addition, the good agreement between experimental results and modeling indicates that determination of binding constants and associated kinetics can be obtained from experimental data by appropriate fit of calculated values.

Acknowledgments

This work was supported by the Natural Sciences and Engineering Research Council of Canada and the Premier Discovery Award. The authors are thankful for initial suggestions on this project from Wennan Zhao and Zhipei Qin from the Department of Chemistry at the University of Waterloo.

Supporting Information

Parameters used for fitting experimental data, coating/solution interface boundary conditions, effect of coating thickness on kinetics, test for boundary layer controlled diffusion, concentration gradients in solution domain, effect of binding rate constants and partition constants on uptake kinetics.

Nomenclature

Symbol	Name

M	Stiff-spring velocity
C_A^s	Analyte concentration in solution
k_f	Association rate constant
k_r	Dissociation rate constant
K_{fs}	Partition coefficient
D_A^s	Diffusion coefficient of analyte in solution
D_A^f	Diffusion coefficient of analyte in fiber
C_B	Bound analyte concentration
D_{BS}	Diffusion coefficient of the complex in solution
b	Diameter of the fiber core
a	Thickness of the fiber coating
ρ	Density of water
μ	Dynamic viscosity of water
R	Radius of the magnetic stirrer
L	Radius of the sample container
t_s	Time scale of analyte diffusion

References

1. Boyaci, E.; Rodriguez-Lafuente, A.; Gorynski, K.; Mirnaghi, F.; Souza-Silva, E. A.; Hein, D.; Pawliszyn, J. *Anal. Chim. Acta* **2015,** *873,* 14-30.

2. Pawliszyn, J. solid phase microextraction: theory and practice. Wiley-VCH: Toronto, 1997.

3. Lao, W.; Maruya, K. A.; Tsukada, D. *Anal. Chem.* **2012,** *84,* 9362-9369.

4. Eijkeren, J. C.; Heringa, M. B.; Hermens, J. L. M. *Analyst* **2004,** *129,* 1137-1142.

5. Vaes, W. H. J.; Ramos, E. U.; Casper, H.; Holsteijn, I.; Blaauboer, B. J.; Seinen, W.; Verhaar, H. J. M.; Hermens, J. L. M. *Chem. Res.Toxicol.* **1997,** *10,* 1067-1072.

6. Heringa, M. B.; Hogevonder, C.; Busser, F.; Hermens, J. L. M. *J.Chromatogr., B: Anal. Technol. Biomed.Life Sci.* **2006,** *834,* 35-41.

7. Heringa M. B. , Hermens. J. L. M. *Trends Anal. Chem.* **2003,** *22,* 575-587.

8. Kopinke, F. D.; Ramus, K.; Poerschmann, J.; Georgi, A. *Environ. Sci. Technol.* **2011,** *45,* 10013-10019.

9. Heringa, M. B.; Pastor, D.; Algra, J.; Vaes, W. H. J.; Hermens, J. L. M. *Anal. Chem.* **2002,** *74,* 5993-5997.

10. Santillo, M. F.; Ewing, A. G.; Heien, M. L. *Anal. Bioanal. Chem.* **2011,** *399*, 183-190.

11. Vulic, K.; Pakulska, M. M.; Sonthalia, R.; Ramachandran, A.; Shoichet, M. S. *J. Controlled Release* **2015,** *197*, 69-77.

12. Louch, D.; Motlagh, S.; Pawliszyn, J. *Anal. Chem.* **1992,** *64*, 1187-1199.

13. Mahmud, T.; Haque, J. N.; Roberts, K. J.; Rhodes, D.; Wilkinson, D. *Chem. Eng. Sci.* **2009,** *64*, 4197-4209.

14. Bird, R. B.; Stewart, W. E.; Lightfoot, E. N. *Transport Phenomena*. 2nd ed.; Wiley & Sons: Toronto, 2002.

15. Datta, A.; Rakesh, V. *An Introduction to Modeling transport processes*. 1st ed.; Cambridge University Press: New York, 2010.

16. Buchwald, P. *Theor. Biol. Med. Model.* **2009,** *6*, 5.

17. Ellis, J. S.; Strutwolf, J.; Arrigan, D. W. *Phys. Chem. Chem. Phys.* **2012,** *14*, 2494-500.

18. Crank, J. *The Mathematics of Diffusion*. 2nd ed.; Clarendon Press: Oxford, 1975.

19. Kramer, N. I.; Eijkeren, J. C. H.; Hermens, J. L. M. *Anal. Chem.* **2007,** *79*, 6941-6948.

20. Broeders, J. J.; Blaauboer, B. J.; Hermens, J. L. M. *J. Chromatogr., A* **2011,** *1218*, 8529-8535.

21. Poerschmann, J.; Zhang, Z.; Kopinke, F. D.; Pawliszyn, J. *Anal. Chem.* **1997,** *69*, 597-600.

22. Reyes-Garces, N.; Bojko, B.; Pawliszyn, J. *J. Chromatogr., A* **2014,** *1374*, 40-49.

23. Ramos, E. U.; Meijer, S. N.; Vaes, W. H. J.; Verhaar, H. J. M.; Hermens, J. L. M. *Environ. Sci. Technol.* **1998,** *32*, 3430-3435.

24. Oomen, A. G.; Mayer, P.; Tolls, J. *Anal. Chem.* **2000,** *72*, 2802-2808.

For TOC only

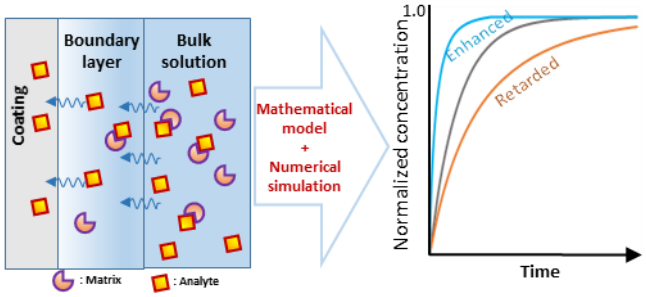
Coating
Boundary layer
Bulk solution
: Matrix
: Analyte
Mathematical model
+
Numerical simulation
1.0
Normalized concentration
Enhanced
Retarded
Time